

APPLICATION OF DIGITAL IMAGE CORRELATION METHOD IN RC AND FRC BEAMS UNDER BENDING TEST

* Aris Aryanto¹, Messa Revolis², Yuki Oribe³ and Hibino Yo⁴

^{1,2} Faculty of Civil and Environmental Engineering, Bandung Institute of Technology, Indonesia; ^{3,4} Graduate School of Engineering, Hiroshima University, Japan

*Corresponding Author, Received: 14 June 2022, Revised: 15 Dec. 2022, Accepted: 10 Jan. 2023

ABSTRACT: Techniques to monitor deformation and strain fields and crack development in experimental testing are continuously improved. Digital Image Correlation (DIC) technique that recently developed several past decades is a powerful tool for measuring object deformation. Using image correlation, this method can correlate the digital images of undeformed and deformed objects to determine the displacement and strain field. Compared to conventional techniques (such as strain gauges), DIC has superiority due to computational accuracy, efficiency, and non-contact measurement. In this study, DIC is applied to analyze the mechanics of plain and fibrous concrete beams under the 4-point bending test in the laboratory. Four beam test specimens were made and tested. Displacement and strain fields derived from digital image correlations are analyzed in crack detection, deflection, and strain of beams. DIC analysis results show good agreement with experimental measurement and are suitable for early crack detection and crack measurement. Monitoring strain fields and cracks using DIC confirms the influence of fiber engagement on load resistance, cracking, and flexural behavior.

Keywords: Digital Image Correlation (DIC), Concrete beams, Strain, Crack

1. INTRODUCTION

Reliable deformation measurement is essential for experimental test measurements in quasi-brittle materials such as concrete structures. The most common conventional technique to measure deformation and strain field is strain gauges attached to the specimen's surface, e.g., concrete or steel reinforcements. However, measuring displacement and strain fields to capture the complete structural behavior requires many gages and will be expensive.

Recently, a method known as Digital Image Correlation (DIC) has been developed to measure deformation and strain variation and cracks on an element's surface plane. This is based on advances in digital technology that capture high-resolution images supported by an advanced computation that can process the data from a digital image correlation [1]. DIC is relatively easy to operate, may reduce experimental costs, and is considered more accurate in results than conventional measurements. It can also be performed for various potential applications and in different types of materials [2]. Furthermore, several open-source and non-commercial DIC processing software are available nowadays [3].

DIC uses a non-contact optical measurement technique that can be applied to the specimen's surface. It requires a continuous digital image that captures during the test. The displacement field is determined from the correlation between two images, undeformed and deformed images. This

method can be applied from a small to a large-scale test. The accuracy of displacement measurement by DIC is highly dependent on image texture or contrast [4,5], and image resolution [6].

There are numerous concrete material and element testing that could be carried out in the laboratory, e.g., compressive strength, tensile strength, or flexural testing. Those testing may utilize DIC technology to measure deformation and strain fields. For example, Tambusay A. et al. [7] Sindu B. S. and Sasmal S. [8], Verbruggen S., et al. [9], and Lacidogna G. et al. [10] use the DIC method for direct tensile and flexural concrete testing. Gali S. and Subramaniam K. V. L. [11] also investigate the formation and propagation of a critical shear crack of beams using the DIC technique.

The application of the DIC method to evaluate fracture mechanisms on various materials was also conducted by several researchers. Bueno J. A. and Lambros J. [12] investigate the fracture of nonhomogeneous materials. The DIC method was implemented using bilinear and bicubic interpolation, and coarse-fine and Newton-Raphson optimization algorithms. Crack opening displacement fields were well captured using DIC. Filho J, Xavier J, and Nunes L. [13] use the DIC method for crack tip detection of fibrous soft composites. Consistent estimation of fracture parameters from DIC and visual inspection approach was obtained.

Fayyad T. M. and Lees J. M [14] and Bhosale

A. B. and Prakash S.S. [15] evaluate fracture properties of reinforced concrete using the DIC technique. It is found that DIC is effective in monitoring crack profiles in small-scale reinforced concrete beams. Meanwhile, Gentruck et al. [16] use DIC for full-scale testing of the prestressed concrete structures.

Moreover, the extent of DIC's capabilities and the accuracy of results still need to be studied and verified. To have good accuracy and to eliminate errors e.g., from lens distortion some methods also have been introduced [17] including the assessment of speckle patterns [18].

In this study, simple DIC instruments with available non-commercial DIC software were introduced to test the specimens under bending testing. The DIC method was used in the 4-point bending testing of beams to evaluate deformation behavior and crack propagation by comparing the results from the conventional instrument readings. Four concrete beams were cast using normal (plain) or fibrous concrete with or without longitudinal reinforcement. As known, fiber's addition to concrete mixture has been known to change the post-cracking behavior of the concrete elements. Therefore, this paper aims to demonstrate the applicability of DIC measurements results to determine the flexural and crack behavior of various beam samples, i.e., plain concrete, fibrous concrete, and concrete with steel bars,

2. RESEARCH SIGNIFICANCE

Digital image correlation (DIC) is a non-destructive and non-contact deformation measurement applying optical measurement and digital image processing technology. It has been frequently used in laboratory testing for deformation measurement of quasi-brittle material such as concrete in recent years. Since the bending test is recommended as a standard method to study the tensile or flexural capacity of fiber-reinforced concrete (FRC) and required deformability evaluation, in this study, bending tests on concrete beam specimens with and without fiber addition are performed, and crack propagation is investigated by DIC method using simple instrumentations. Crack and deformability evaluation from the DIC results shows a good agreement with the conventional measurements.

3. EXPERIMENTAL PROGRAM

3.1 Specimen Detail

Four concrete beams were cast and tested to investigate load deformation and crack behavior. All beams have similar dimensions, specified concrete strength, and loading arrangement but

differ in fiber and longitudinal reinforcement addition. Polypropylene fiber with a 0.5% of volume fraction was used in this experiment. Specified concrete strength is 60 MPa, and the average measured concrete strength from compressive testing is 62 MPa for normal concrete (NC) and fiber concrete (FC).

This study uses a deformed steel bar with a nominal diameter of 13 mm with a specified yield strength of 400 MPa (BJD40). All specimens tested in this study are summarized in Table 1. Fig.1 below shows the beam dimensions and reinforcement details.

Table 1 Specimen details

Specimen	Concrete type	Deformed steel bars
NC	Plain	No
FC	Fiber	No
NC-S	Plain	2D13
FC-S	Fiber	2D13

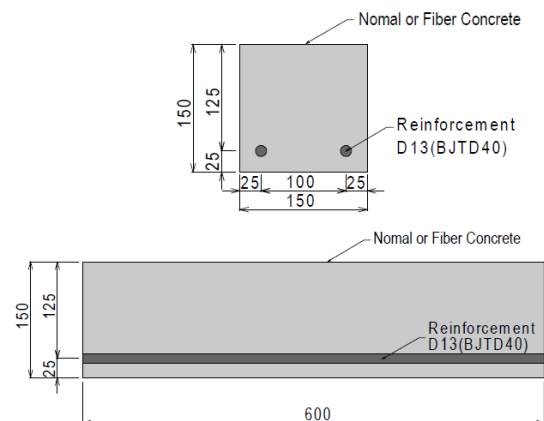


Fig.1 Beam dimensions (in mm)

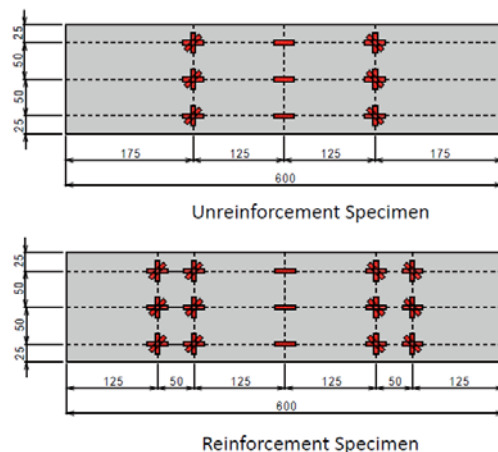


Fig.2 Strain gages setup configurations

To evaluate the strain and curvature in concrete beams, the strain gauges were attached to the surface of one side of the shaft, and another surface side was used as a surface object for DIC measurement. Strain gages configuration is shown in Fig. 2 for unreinforced and reinforced beam specimens.

3.2 DIC and Test Setup

All specimens were tested using a four-point bending test. Each beam was supported at both ends by two roller supports. The two-roller support was kept to have a clear distance of 450 mm. The load was applied at two-point that have a distance of 150 mm from each support. The beams were loaded using a universal testing machine (UTM) with displacement control. Three linear variable displacement transducers (LVDT) were installed under beams at 1/3, 1/2 (midspan), and 2/3 of the beam span to measure the deflection. A micro-camera with the crack width measurement was used to measure the crack opening.

A DLSR camera with a maximum image resolution of 5184 x 3456 pixels and a focal length of 55 mm was used to record the digital images under loading (Fig. 3). The camera was put on a tripod and fixed away from the specimen and has a perpendicular axis to the surface of interest. Surface displacements were obtained by DIC using digital image cross-correlation. The image must have a particular texture from speckle patterns. To have speckle patterns, one surface of the beams was sprayed by applying a uniform white paint followed by a mist of black paint from the spray nozzle (Fig. 4). The speckle patterns were created on the side without strain gauge attachment.

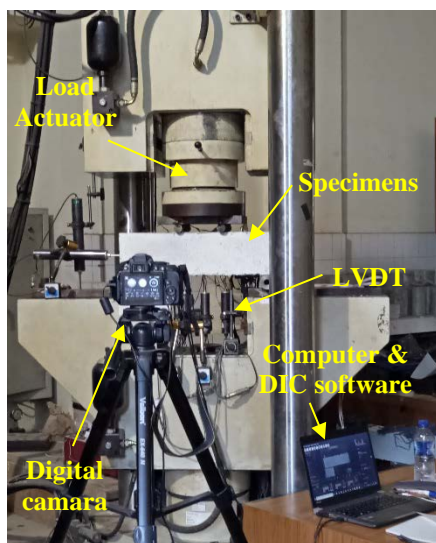


Fig.3 DIC and loading test setup



Fig.4 Speckle making and pattern

4. RESULTS AND DISCUSSIONS

4.1 Displacement Fields

Fig. 5 shows the displacement fields of the NC specimen, plain concrete beam without fiber and steel bar, at an initial, 27.76 kN, and 31.8 kN of loading conditions. The color shows the intensity of displacement.

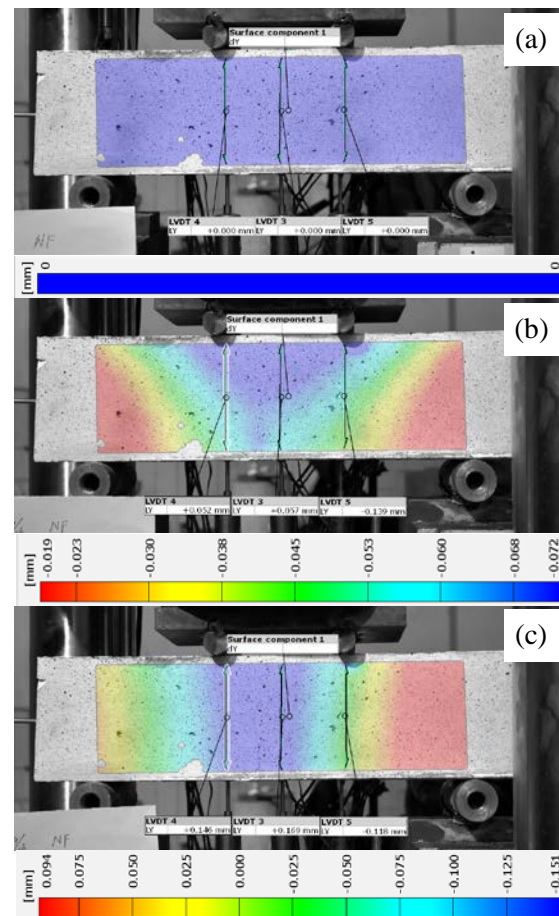


Fig.5 Displacement fields of beams of NC at load (a) 0 kN (c) 27.76 kN (d) 31.8 kN

From the displacement field contour, as shown in Fig.5, at the lower load a localized deformation near the load point is identified and forms a V-pattern of displacement fields. For larger load displacement fields, it forms a vertical uniform intensity over the height of beams and gradually changes from support to midspan of beams.

Displacement fields for all specimens at failure are shown in Fig. 6. The displacement fields contour is almost similar for all specimens except when a large flexural crack occurred the displacement fields could not be monitored and measured near the cracking zone. In addition, when the shear crack occurred, a drastic color change near the shear crack was also identified.

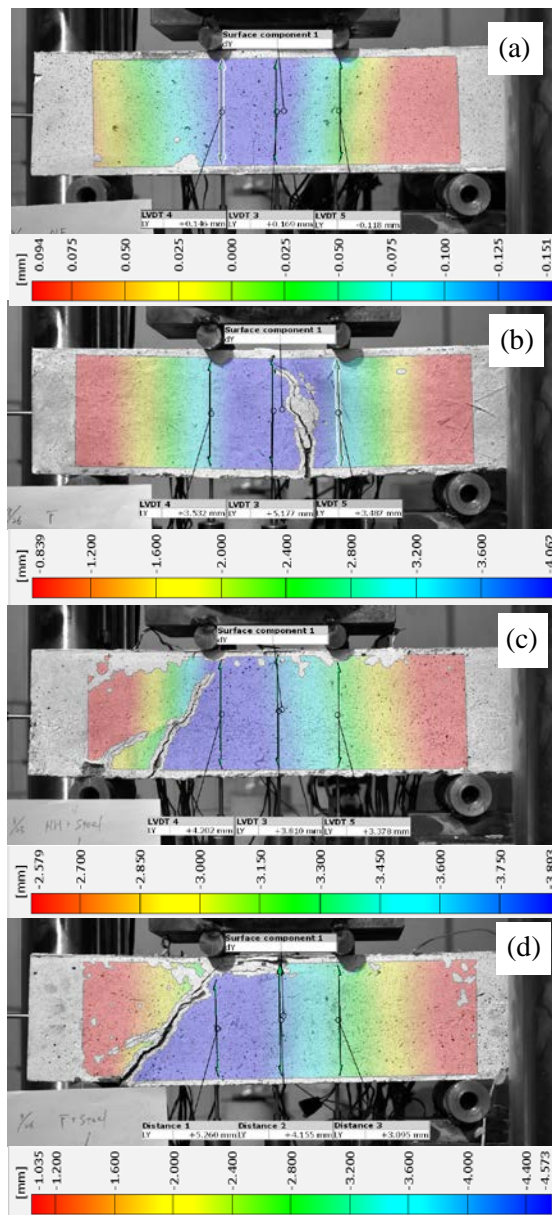


Fig.6 Displacement fields of beams (a) NC (b) FC (c) NC-S (d) FC-S at failure

4.2 Load-Deflection Relationship

Beam's load-deflection responses are shown in Fig.7. Measured beam deflections shown in the figure are obtained at the midspan location. Beams' load capacity increases with the presence of fibers and longitudinal bars. The load response could not be controlled after the peak load in a beam without fibers and steel bars (NC), even with displacement control. With fiber addition in the concrete beams (FC and FC-S), there is an increase in load capacity indicated by a higher peak load. The peak load and corresponding deflections of all beams are listed in Table 2. The post-peak load response in fiber concrete beams showed a larger deflection than in non-fibers concrete beams. In FC specimens, beam with fibers and without longitudinal bars, there is a second peak load after the first peak or cracking load. This indicates that fibers significantly affect post-cracking behavior as crack-bridging increases deformation and toughness capacity. As shown in Fig.7(b) for FC-S specimens, there is no second peak load. However, there is a steady decrease, almost constant, in the load with increasing deflection. The effect of fibers is also noticed when comparing the peak load with the beam without fibers (NC-S).

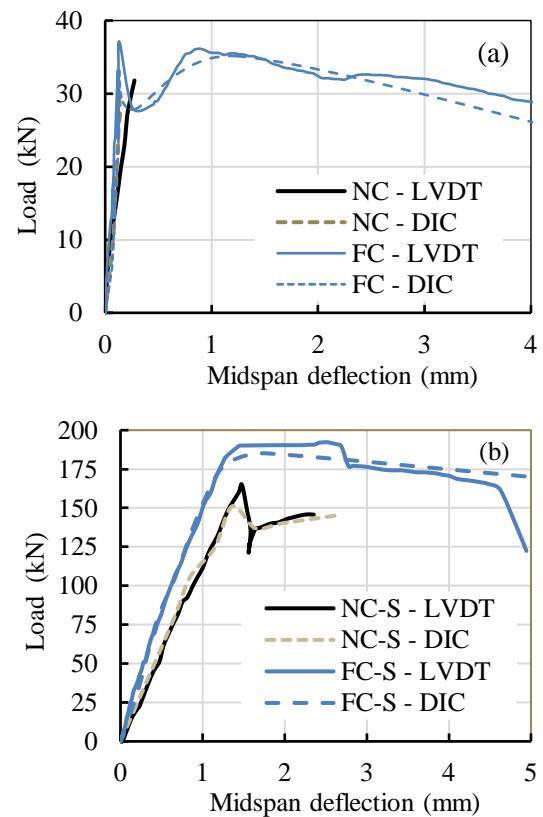


Fig.7 Load-deflection responses of beams (a) NC vs. FC (b) NC-S vs. FC-S

Table 2 Summary of beam test

Specimen	Peak Load (kN)	Percent increase in peak load	Mode of failure
NC	31.8	-	Flexure
FC	35.12	27.6%	Flexure
NC-S	145.7	-	Shear
FC-S	185.08	27%	Shear

Note: comparison was made only between non-fiber and fiber concrete.

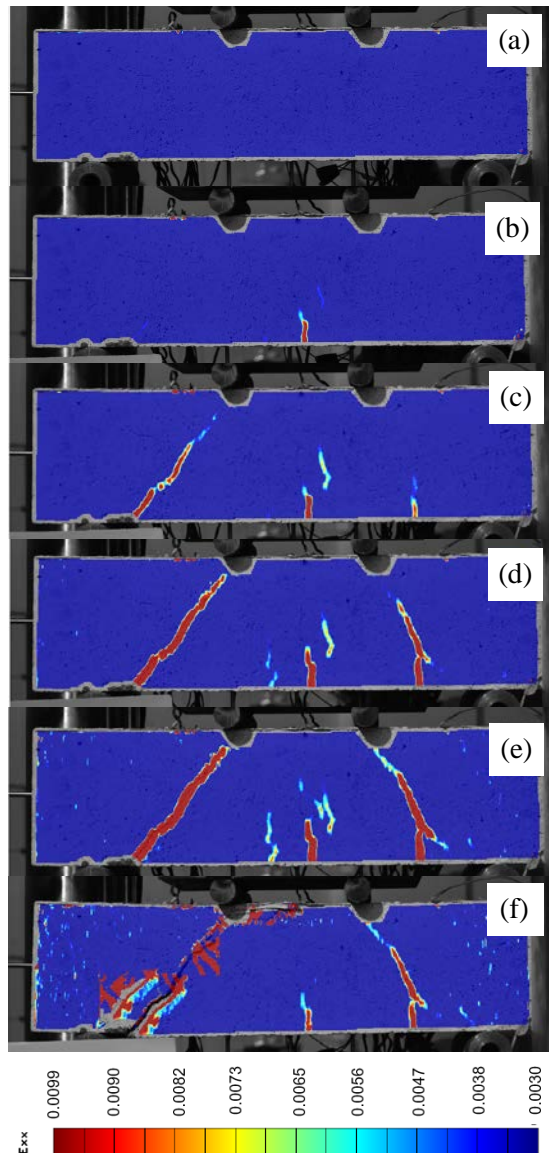


Fig. 8 Strain contours of FC-S beam at loads (a) 35.26 kN (b) 77.14 kN (c) 106.05 kN (d) 139.37 kN (e) 185.08 kN (f) failure.

The images taken under different load conditions were analyzed using DIC software for each beam specimen using cross-image correlations. The displacement vectors of the DIC analysis results determined the beam deflection and crack opening. The displacement value from the DIC analysis was verified against the displacement from LVDTs. As shown in Fig. 7, the DIC approach effectively measures the displacement of beam elements and does not much differ from the LVDT measurements.

4.3 Crack Pattern and Crack Progression

DIC was used to evaluate the beam's crack pattern and crack progression. Measured strain fields in the horizontal direction were used to identify the crack pattern and progression on the concrete beam surface. To identify cracks in the surface, a localized swarm of strain contours in a small region may indicate the crack. The crack pattern and the cracking sequence can be observed using this procedure. The DIC analysis results have more accurate than the visual observation indicated by the detection of a crack identified at a lower load compared to visual observation as shown in Fig.8 (b).

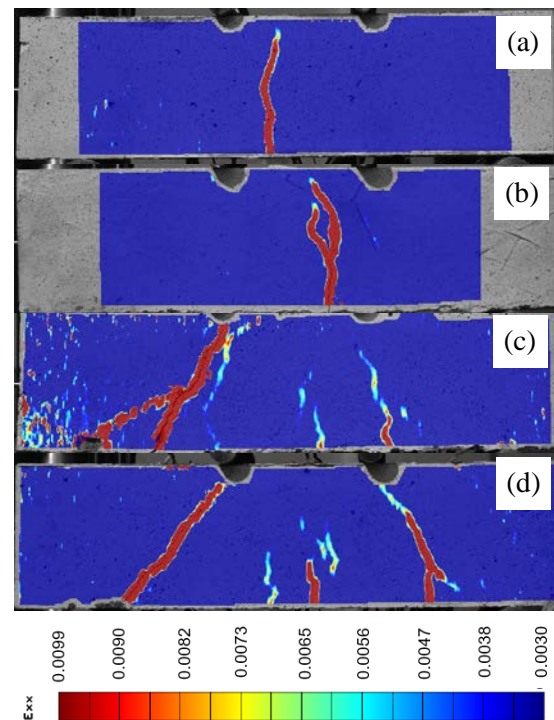


Fig. 9 Strain contours at peak load of beams: (a) NC (b) FC (c) NC-S (d) FC-S.

The formation and progression of cracks in beams with fibers and longitudinal bars (FC-S) are shown in Fig. 8 (a-f).

A flexural crack was initiated in the middle of the beam at a load of 35.26 kN (Fig. 8 (a)). Then, a shear crack located near the support was formed, as shown in Fig. 8(c). The shear crack was formed at approximately 45 degrees of the height of the beam. Then another shear crack that originated from the flexural crack was also developed. This shear crack extended to the load point and became a primary failure mode. The failure mode of beams is a shear failure due to additional longitudinal bars that increase the flexural capacity. All beams without longitudinal steel bars fail in flexure.

Comparing FC-S and NC-S, a beam without fibers (NC-S) not only exhibits shear cracking but also experiences bond-splitting cracking, as shown in Fig. 9 (c). This is also identified in the load-deflection response in Fig.7 (b) that the beam exhibits small deformability. This also indicates that fiber addition significantly increases the bond-

splitting capacity of beams. DIC results can generally capture the crack pattern and progression, which is essential for evaluating structural behavior and failure mode.

The crack patterns at the peak load for all beams are shown in Fig. 9. It is demonstrated that the critical crack patterns, e.g., shear, flexure, and bond splitting cracks that lead to failure, can be identified through DIC analysis.

4.4 Crack Opening Measurement

Crack opening of shear and flexural cracks were measured at several locations in the primary crack, as shown in Fig. 10. Fig. 10 indicates the beam's crack opening calculated using DIC and crack meter methods under different loading rates. The crack opening was measured through field displacements from the DIC analysis. Cracks can be identified

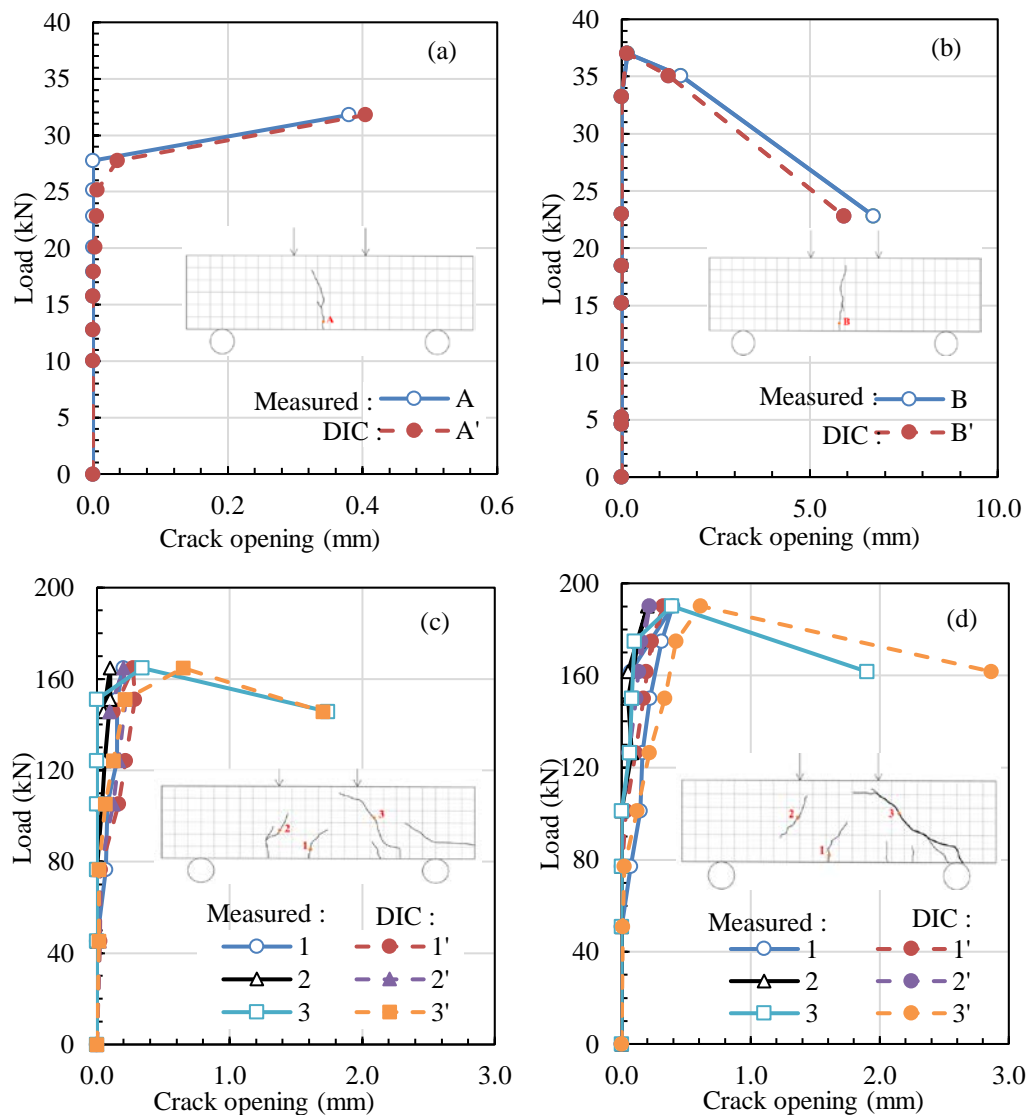


Fig. 10 Crack opening with manual and DIC measurement (a) NC (b) FC (c) NC-S (d) FC-S.

accurately from displacement contours after crack formation and can be observed much earlier than visual observation. A pair of gauge points were placed on either side of the crack to evaluate the displacement across the crack. The line joining the gauge points should be perpendicular to the crack lines. The gauge points should be set in fixed positions in processing digital images at different loads then the horizontal and vertical displacements will be obtained. The crack opening was obtained from relative displacement between two-gauge points across the crack.

The crack width openings measured across the primary crack from all beams are shown in Fig. 10. As shown in Fig. 10 measured crack width using the DIC method has a good agreement with manual measurements. With the addition of fibers in unreinforced beams, there is a delay in flexural crack formation indicated by a higher load when compared to a normal concrete beam (NC). It also shows an increase in crack width opening throughout the load response. Fiber addition for reinforced beams that fail in shear affects the crack opening, which continues to open even in the post-peak as the load decreases. This indicates that fibers control the shear crack opening or dilatancy, which may lead to an alternate failure mode. A normal beam without fibers (NC-S) leads to bond splitting failure as a horizontal crack formed at the longitudinal bar axis near the support.

5. CONCLUSION

Digital image correlation (DIC) in this study is used to observe deformation, crack patterns, crack progression and crack opening of all beam specimens under the bending test. From this limited investigation, some conclusions can be drawn.

- DIC produces reasonable displacement fields and closely load-deflection curves compared to LVDT measurements. The beam's load-carrying capacity and ductility increase with fiber addition, indicated by peak load and post-peak displacement from load-deflection responses.
- The DIC method effectively determines the crack pattern and progression in the bending test of unreinforced and reinforced concrete beams with or without fiber addition. Using the DIC method, the failure mode of beams can be captured from the crack pattern and crack progression. Unreinforced beams (NC and FC) exhibit flexural failure, and reinforced beams (NC-S and FC-S) produce shear failure.
- The crack opening at selected locations in the beams extracted from DIC analysis was used to evaluate the effect of fiber addition and longitudinal bars as beam parameters. Fiber addition affects the crack opening, which can

continue to grow even in the post-peak as the load decreases. Fibers in concrete seem to play a role in the crack progression and crack bridging.

6. ACKNOWLEDGMENTS

This study is part of a research collaboration program between Bandung Institute of Technology (ITB), Indonesia, and Hiroshima University, Japan. Support from both institutions is acknowledged.

7. REFERENCES

- [1] Supriya S. Gadhe S.S. and Navthar R. R., Digital Image Correlation Technique for Strain Measurement of Aluminum Plate, *International Journal of Engineering Trends and Technology*, Vol. 39, Issue. 6, 2016, pp.306-311.
- [2] McCormick N. and Lord J., Digital Image Correlation, *Materials Today*, Vol.13, Issue. 12, 2010. pp.52-54.
- [3] Belloni V., Ravanelli R., Nascetti A., Di Rita M. Mattei D., and Crespi M., py2DIC: A New Free and Open-Source Software for Displacement and Strain Measurements in the Field of Experimental Mechanics, *Sensors*, Vo.19. 3832, 2019. pp. 1-19.
- [4] Mauroux T., Benboudjema F. Turcry P., Aït-Mokhtar A., and Deves O., Study of Cracking Due to Drying in Coating Mortars by Digital Image Correlation, *Cement and Concrete Research*, Vol. 42, No. 7, 2012, pp. 1014-1023.
- [5] Lecompte D, Smits A., Bossuyt S., Sol H., Vantomme J., Van Hemelrijck D., Habraken A.M., Quality assessment of speckle patterns for digital image correlation, *Optics and Lasers in Engineering* Vol. 44,2006, pp. 1132–1145.
- [6] Sun Z., Lyons J. S., and McNeill S. R. Measuring Microscopic Deformations with Digital Image Correlation, *Optic, and Lasers in Engineering* Vol. 27, 1997, pp. 409-428.
- [7] Tambusay A., Suryanto B., and Suprobo P., Digital image correlation for cement-based materials and structural concrete testing, *Civil Engineering Dimension* Vo.22. No.1, 2020, pp.6-12.
- [8] Sindu B. S., and Sasmal S., Multi-scale Abridged Cement Composite with Enhanced Mechanical Properties, *ACI Materials Journal*, Vol. 117, No. 4, 2020, pp.105-117
- [9] Verbruggen S., DeSutter S., Iliopoulos S., Aggelis D.G., and Tysmans T., Experimental structural analysis of hybrid composite-concrete beams by digital image correlation (DIC) and acoustic emission (AE), *J. Nondestructive Eval.*, 35, 2016, pp. 1-10
- [10] Lacidogna G., Piana G., Accornero F., and Carpinteri A., Multi-technique damage

- monitoring of concrete beams: acoustic emission, digital image correlation, dynamic identification, *Constr. Build. Mater.*, 242, 2020, pp.1-18
- [11] Gali S. and Subramaniam K. V. L., Shear behavior of slender and Non-slender Steel Fiber- Reinforced Concrete Beams, *ACI Structural Journal*, Vol. 116, No. 3, 2019, pp.149-158.
- [12] Bueno J. A. and Lambros, J., Investigation of crack growth in functionally graded materials using digital image correlation, *Engineering Fracture Mechanics*, 69, 2002, pp.1695-1711.
- [13] Filho J, Xavier J, and Nunes L., An alternative digital image correlation-based experimental approach to estimate fracture parameters in fibrous soft materials. *Materials*;15(7). 2022, pp.1-12.
- [14] Fayyad T. M. and Lees J. M., Application of Digital Image Correlation to reinforced concrete fracture, *Procedia Materials Science*, 20th European Conference on Fracture (ECF20), 2014, pp. 1585 – 1590.
- [15] Bhosale A. B. and Prakash S.S., Crack Propagation Analysis of Synthetic vs. Steel vs. Hybrid Fibre-Reinforced Concrete Beams Using Digital Image Correlation Technique, *Int J. Concr. Struct. Mater.*, Vol 14:57, 2020, pp.1-19.
- [16] Genctrurk B., Hossain K., Kapadia A., Labib E., Mo Y. Use of digital image correlation technique in full-scale testing of prestressed concrete structures, *Measurement* Vol. 47, 2014, pp. 505-515.
- [17] Pan B., Yu L., Wu D., and Tang L, Systematics errors in two-dimensional digital image correlation due to lens distortion, *Optics, and Laser in Engineering*, 21, 2012, pp.140-147.
- [18] Lecompte D., Smits A., Bossuyt S., Sol H., Vantomme J., Van Hemmelrijck D., and Habraken A.M., Quality assessment of speckle patterns for digital image correlation, *Optics and Laser Engineering*, 44, 2006, pp.1132-1145.

Copyright © Int. J. of GEOMATE All rights reserved,
including making copies, unless permission is obtained
from the copyright proprietors.
